

Investigation of the Local Structure of Mixtures of an Ionic Liquid with Polar Molecular Species through Molecular Dynamics: Cluster Formation and Angular Distributions

Jesús Carrete,[†] Trinidad Méndez-Morales,[†] Óscar Cabeza,[‡] Ruth M. Lynden-Bell,[§] Luis J. Gallego,[†] and Luis M. Varela^{*,†}

[†] Grupo de Nanomateriais e Materia Branda, Departamento de Física da Materia Condensada, Universidade de Santiago de Compostela, Campus Vida s/n E-15782, Santiago de Compostela, Spain

[‡] Facultade de Ciencias, Universidade da Coruña, Campus A Zapateira s/n E-15008, A Coruña, Spain

[§] Department of Chemistry, University of Cambridge, Lensfield Road, Cambridge, United Kingdom CB2 1EW

Supporting Information

ABSTRACT: In this work, we used molecular dynamics simulations to analyze in detail the spatial distributions of the different constituents in mixtures of 1-butyl-3-methylimidazolium tetrafluoroborate with three polar molecular species: water and two alcohols of different chain lengths (methanol and ethanol). In particular, we report results regarding the influence of the chosen species and its concentration on the formation of ionic and molecular clusters over the whole miscibility range, as well as on the angular distribution of polar molecules around the anion and the cation in these systems. Both analyses showed that addition of a molecular species breaks down the polar network of the pure ionic liquid in clusters whose mean size decreases progressively as more molecules are added. At very high concentrations of the molecular species, the ions are found to be isolated in mixtures with water and methanol, but they tend to form pairs in ethanol. In mixtures with water we identified large clusters that form a water network at very high water concentrations, while at low water concentrations polar molecules tend to form smaller aggregates. In contrast, in mixtures with alkanols there is no evidence of the formation of large alcohol clusters at any concentration. Spatial order in alcohol was also studied by means of the Kirkwood G factor, reaching the conclusion that the angular correlations which appear in pure alcohols due to dipole interactions are destroyed by the ionic liquid, even when present only in tiny amounts.



INTRODUCTION

In the past few years, room-temperature ionic liquids (ILs) have been widely investigated due to their unique properties, such as vanishing vapor pressure, wide thermal and electrochemical stability, low viscosity, high ionic conductivity, and their power to dissolve a wide range of substances.^{1–4} These attributes, together with the multiple possible combinations of cations and anions,⁵ contribute to their consideration as a “green” alternative to traditional organic solvents^{4,6–8} and to their use in a number of technological applications.^{9–11}

The most extensively studied class of ILs is that based on the 1-alkyl-3-methylimidazolium ($[\text{AMIM}]^+$) cation combined with various anions like $[\text{PF}_6]^-$, $[\text{BF}_4]^-$, $[\text{NTf}_2]^-$, etc.¹⁰ The choice of cation and anion can affect the miscibility with other species such as water or alcohols; for example, the solubility of imidazolium-based ILs in water decreases with an increase in the length of the alkyl side chain,¹² while the behavior in mixtures with an alcohol is exactly the opposite.^{12,13} The relation of the miscibility behavior with a variation of the anion is more complex but, in general, solubility is higher for smaller anions.¹⁴ The presence of these molecular species can completely change several physical and chemical properties of

ILs such as polarity, viscosity, electrical conductivity and solubility.^{15–17} Therefore, an insight at the molecular level into the properties of mixtures of ILs with species such as water or alcohols is of primary importance from both theoretical and industrial perspectives.

The presence of water in ILs is very common since all of them are hygroscopic (even hydrophobic ILs can absorb a significant amount of water from the atmosphere).^{3,10,18,19} Because of this reason, a large number of both experimental^{20–23} and computational^{24–29} studies of the nanostructural organization of ILs when mixed with water and of the interactions between them can be found in the literature. However, studies concerned with mixtures of ILs with alcohols have been scarcer and, to our knowledge, only our previous paper³⁰ about molecular dynamics (MD) simulations of mixtures of 1-hexyl-3-methylimidazolium hexafluorophosphate ($[\text{HMIM}][\text{PF}_6]$), 1-hexyl-3-methylimidazolium tetrafluoroborate ($[\text{HMIM}][\text{BF}_4]$) and 1-hexyl-3-methylimidazolium chlor-

Received: February 9, 2012

Revised: May 4, 2012

Published: May 15, 2012



ide ($[HMIM][Cl]$) with ethanol and methanol deals, albeit indirectly, with the evolution of cluster formation with alcohol concentration. However, the work by Canongia-Lopes et al.³¹ in which they performed a structural analysis of the solvation of polar, nonpolar and associating molecular species in 1-butyl-3-methylimidazolium hexafluorophosphate $[BMIM][PF_6]$ at 330 K, including methanol and water among their chosen molecular species must also be mentioned, since in it they address the microsegregation of polar and apolar domains and include water and methanol among their choices of molecular species.

Among the experimental studies reported up to now, Fazio et al.²¹ investigated, by using Raman and infrared spectroscopy, the local organization of water in mixtures with 1-butyl-3-methylimidazolium tetrafluoroborate ($[BMIM][BF_4]$). They indicated that at very high concentrations of IL water molecules tend to be isolated from each other or exist as small independent clusters embedded in the polar network. They proposed a picture where, as water concentration increases, a continuous water network appears and coexists with the IL. That same year, Zhang et al.²³ applied two-dimensional vibrational spectroscopy to investigate the dilution process of 1-ethyl-3-methylimidazolium tetrafluoroborate ($[EMIM][BF_4]$) in water. They found that the network formed by cations and anions in pure ILs is gradually split into huge ionic clusters, and then those are further dissociated into ionic pairs surrounded by water.

Regarding computational studies, up to our knowledge the first molecular description of water structuring within an IL was provided by Hanke and Lynden-Bell.²⁴ They performed MD simulations of mixtures of 1,3-dialkylimidazolium ILs and water in order to investigate their microscopic physical properties as a function of composition. They reported that water molecules tend to be isolated from each other in mixtures with fewer water molecules than ions, while at high water concentrations a percolating network of water coexists with some isolated molecules and small clusters of this species. Last year, Bernardes et al.²⁵ performed MD simulations of the structure of aqueous solutions of 1-ethyl-3-methylimidazolium ethylsulfate ($[EMIM][EtSO_4]$) in the entire concentration range. They described the size and connectivity of different water and ion aggregates as a function of the concentration of water, identifying four concentration ranges with distinct structural regimes and two different percolation thresholds. As regards the work by Canongia-Lopes et al.,³¹ they showed that the nature of ILs as solvents microsegregated between polar and apolar domains influences the solvation process in these media. For example, in the methanol and water solutions they report about, molecule–anion interactions were found to be very similar and dominated by hydrogen bonding, while with respect to molecule–cation interactions water was concentrated in the charged domain and methanol interacted with both apolar and charged domains. Another useful way of gathering information about the microscopic structure of these mixtures is the study of the angular distribution of the molecules. Spickermann et al.²⁹ presented results from a first-principles MD simulation of a single 1-ethyl-3-methylimidazolium chloride ($[EMIM][Cl]$) ion pair dissolved in 60 water molecules. They studied the orientation of water molecules within the solvation shells and they found evidence for a linear hydrogen bond arrangement from chloride to water, in contrast to a tangential orientation of water around the hydrophobic subgroups.

In spite of these experimental and computational studies on mixtures, our knowledge of the interaction between the IL and

the molecular species, as well as of the aggregation process in the mixture, remains somewhat empirical. In this work we simulated mixtures of $[BMIM][BF_4]$ with three different polar molecular species, water, methanol and ethanol, at several concentrations over the whole miscibility range. Our choice of $[BF_4]^-$ for the anion responds to its displaying an intermediate hydrophobicity between that of halogens and $[PF_6]^-$, in addition to being one of the most popular choices in practical applications. We focused on the study of the formation of ionic and molecular clusters in all the systems, as well as on the structural changes brought about by variations in the molar fractions. Moreover, we analyzed the angular distribution of the polar molecules around the cation and the anion in order to gain insight into their relative orientations.

The remainder of this paper is organized as follows. In the following section we describe the computational procedure employed in this work; next, we present and discuss the results obtained, and in the final part, we summarize our main conclusions.

SIMULATION DETAILS

The MD simulations for pure $[BMIM][BF_4]$ and its mixtures with water and alcohol were performed using version 4.5.4 of the GROMACS package.³² All the simulations were run at 298.15 K, with molar percentages of the molecular species equal to $\%_s = \{0, 5, 15, 25, 50, 75, 80, 85, 90, 95, 98, 99\}$ and 100%. We note that water and both of these alcohols are totally miscible with $[BMIM][BF_4]$ at room temperature.^{33–36} The initial configurations were obtained by randomly placing 300 ionic pairs in the cubic box, except for $\%_s = 100$, a case in which only molecules are present, $\%_s = 95\text{--}99$, where only 50 IL molecules were introduced so as to keep the system size small enough, and $\%_s = 5$, where we considered 950 ionic pairs in order to have enough molecular species to yield statistically significant trajectories. The number of molecules was calculated for each situation by considering each ionic pair as a single unit in the calculation of mole fractions.

The parametrization of the ions was carried out in the framework of the all-atom version of the OPLS force field (OPLS-AA), developed by Jorgensen and co-workers³⁷ for different organic liquids, in which every hydrogen atom bonded to carbon is modeled explicitly. The functional form of the OPLS force field includes intramolecular interactions such as bond stretching, angle bending, dihedral torsion, as well as van der Waals and Coulombic interactions:

$$\begin{aligned} E = & \sum_i K_{b,i} [r_i - r_{0,i}]^2 + \sum_i K_{b,i} [\theta_i - \theta_{0,i}]^2 \\ & + \sum_i \left[\frac{1}{2} V_{1,i} (1 + \cos(\varphi_i)) + \frac{1}{2} V_{2,i} (1 - \cos(2\varphi_i)) \right. \\ & \left. + \frac{1}{2} V_{3,i} (1 + \cos(3\varphi_i)) + \frac{1}{2} V_{4,i} (1 - \cos(4\varphi_i)) \right] \\ & + \sum_i \sum_{j < i} \left\{ \frac{1}{4\pi\epsilon_0} \frac{q_i q_j e^2}{r_{ij}} + 4\epsilon_{ij} \left[\left(\frac{\sigma_{ij}}{r_{ij}} \right)^{12} - \left(\frac{\sigma_{ij}}{r_{ij}} \right)^6 \right] \right\} \end{aligned} \quad (1)$$

The parameters required in order to use the above equation are the force constants K , the equilibrium values r_0 and θ_0 , the Fourier coefficients V , and the partial atomic charges q . σ_{ij} and ϵ_{ij} represent the Lennard-Jones (LJ) radii and potential well

depths, respectively, which are obtained from parameters for each type of atom using the geometric combination rules $\epsilon_{ij} = (\epsilon_i \epsilon_j)^{1/2}$ and $\sigma_{ij} = (\sigma_i \sigma_j)^{1/2}$. The cation was modeled using the all-atom representation of the CH_2 and CH_3 groups in the alkyl chain, as well as that of the methyl group attached to the imidazolium ring. As for the anion, $[\text{BF}_4]^-$ was modeled as a set of five sites with partial charges of 1.176 for the boron atom and -0.544 for the fluorine atoms.³⁸ These partial charges were computed using MP2/6-31g(d) by means the CelpG methodology³⁹ as implemented in the GAUSSIAN⁴⁰ package. On the other hand, water molecules were represented using the TIPSP water model,⁴¹ which consists of a LJ center placed on the oxygen, two positive +0.241 charges located at the hydrogen atoms and two partial -0.241 charges representing the lone pairs of the oxygen atoms; while for ethanol and methanol we employed the molecular model proposed by Jorgensen.⁴² Long-range electrostatic interactions were computed using the particle-mesh Ewald (PME)⁴³ method with a grid spacing of 0.12 nm and cubic interpolation. A cutoff distance of 1.1 nm was used for LJ interactions, a neighbor search was carried out up to this same distance from the central ion, and its results updated every five simulation steps. The linear constraint solver (LINCS) algorithm^{44,45} with a fourth-order expansion of the coupling matrix was used to constrain the bonds, and long-range dispersion corrections were applied to energy and pressure.

Initial configurations were energy-minimized for 10^6 steps using a conjugated gradients algorithm in order to remove bad contacts resulting from the initial random configuration of ions. The maximum step size and the tolerance were set to 0.01 nm and 0.1 kJ/(nm·mol), respectively. The equilibration phase was performed in the isothermal-isobaric (N, p, T) ensemble for a length of 100 ps, which is usually considered to be enough for imidazolium-based ILs.⁴⁶ The results of an additional 2000 ns-long simulation in the isothermal-isobaric ensemble were used for analysis. The temperature control was implemented using the V-rescale thermostat.⁴⁷ Cations and anions (and water or alcohols, when they were included) were separated in two (three) baths with temperature coupling constants of 0.1 ps. Pressure was controlled using the Parrinello-Rahman barostat⁴⁸ with a reference pressure of 1 atm, an isothermal compressibility of 4.5×10^{-5} bar⁻¹, and a relaxation time of 0.1 ps.

Each of these simulations provided us with a sequence of configurations, i.e., positions and instantaneous velocities of all atoms of the system, which was then analyzed so as to obtain structural information about the aforementioned mixtures.

RESULTS AND DISCUSSION

In order to investigate cluster formation when a molecular liquid is added to $[\text{BMIM}][\text{BF}_4]$, we analyzed the size of both ionic and molecular clusters. Following the criterion defined by Hanke and Lynden-Bell²⁴ and later employed by Bernardes et al.,²⁵ we considered that two molecules of water or alcohol are connected to each other and thus belong to the same cluster if the distance between their oxygen atoms is smaller than the radius corresponding to the first minimum in the oxygen–oxygen radial distribution function [RDF, $g(r)$] in the pure liquids (Figure 1, bottom). This is the limit of the first solvation layer, and corresponds approximately to the distance used to define a hydrogen bond in the geometrical criterion commonly employed in MD (hydrogen–acceptor distance smaller than 3.5 Å, and donor–hydrogen–acceptor angle less than 30°).⁴⁹

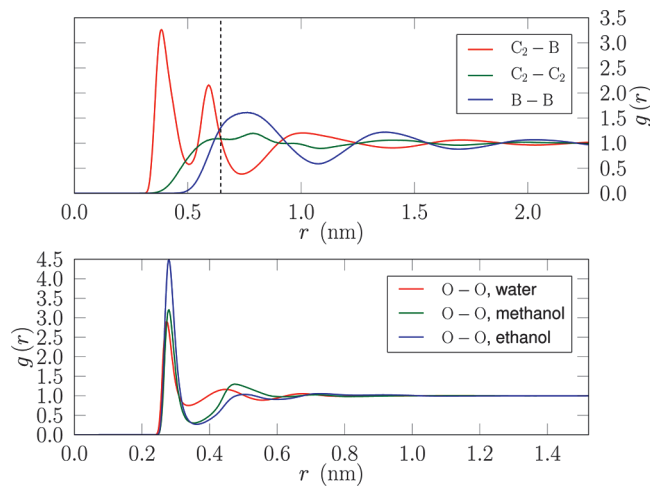


Figure 1. Top: cation–anion, cation–cation, and anion–anion RDFs in pure $[\text{BMIM}][\text{BF}_4]$. The dashed line marks the cutoff distance taken for considering two ions as connected. Bottom: oxygen–oxygen RDFs in pure water, ethanol, and methanol.

The criterion used to define ionic clusters is slightly different. Heterocoordination between cations and anions is the norm in ILs due to its energetic advantages; therefore, the distance considered as the cutoff is 0.65 nm, which is the distance where the cation–anion and cation–cation RDFs of pure $[\text{BMIM}][\text{BF}_4]$ intersect (Figure 1, top), and accordingly the minimum distance at which it is more likely to find a second cation after a cation–anion pair. These RDFs were calculated using the boron atom (B), at the center of mass of $[\text{BF}_4]^-$, as representative of the anion, and the carbon atom between the two nitrogens (C2) as representative of the imidazolium ring. It should be noted that these cutoff distances remain unaffected when the mole fractions are varied.

For each frame along the MD trajectory, a search was performed to build the connectivity matrix of an undirected network representing the neighborhood relations of molecules or ions in the mixture at that particular time step, according to the cutoff radii previously decided on. Clusters were then defined as the connected components of that undirected graph. The cluster distribution of each mixture was obtained by taking into account the clusters formed at all time steps in the simulation. We arbitrarily defined big clusters, for the purposes of the present work, as those which comprise more than 50% of the particles of the class under study (either molecules or ionic pairs) in the simulation box.

Figure 2 shows the evolution of the percentage of water, ethanol and methanol molecules, respectively, that belong to a cluster (i.e., that are not isolated) and to a big cluster. The horizontal axis represents the mole fraction of the molecular species in the mixture. This quantity is calculable *a priori* and gives a direct idea of the number of particles of each type with which an ion or a molecule can interact, but since the volume available to each particle also plays an important role in determining the possible spatial configurations of the system, a representation of the same variable in terms of volume fraction is a useful complement to these plots; see Figure 5 and the associated discussion below. As Figure 2 (top left) shows, all the ions belong to big clusters up to a water molar percentage of 90%; after this concentration the number of cations and anions forming clusters decreases when the amount of water is increased. However, in mixtures with methanol and ethanol

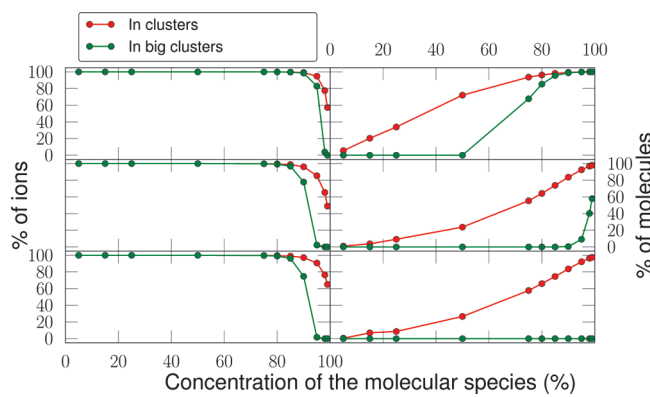


Figure 2. Concentration dependence of the percentage of ions (left panels) and molecules (right panels) forming clusters and big clusters in mixtures of [BMIM][BF₄] with water (top), methanol (center), and ethanol (bottom). Solid circles mark the simulated concentrations; lines are only provided as a guide to the eye. See also Figure 5.

[Figure 2 (center left and bottom left, respectively)] the percentage of ions in big clusters starts to decrease at an alcohol concentration of 80%. In regard to molecular clusters, the percentage of water molecules that belong to a cluster increases rapidly with the amount of water [Figure 2 (top right)]: indeed, at a molar percentage of approximately 35% half of the water molecules belong to a cluster and when 80% of water is reached, more than 80% of the water molecules are forming big clusters. The behavior of alcohol molecules is markedly different: first, the increase with alcohol concentration of the number of molecules belonging to a cluster [Figure 2 (center right and bottom right)] is much slower than in the case of water. Even at 70% alcohol, half of the alcohol molecules still do not belong to any cluster. Methanol molecules start to form big clusters in a significant number at very high alcohol concentrations (99% and above) but these clusters are conspicuously absent from [BMIM][BF₄] + ethanol mixtures.

Further insight into the modifications introduced by a molecular species in the clustering process of [BMIM][BF₄] is given by the size distribution histograms of ionic and molecular clusters for each of the systems. In Figure 3, we illustrate the probability of finding an ion or a molecule of water in an

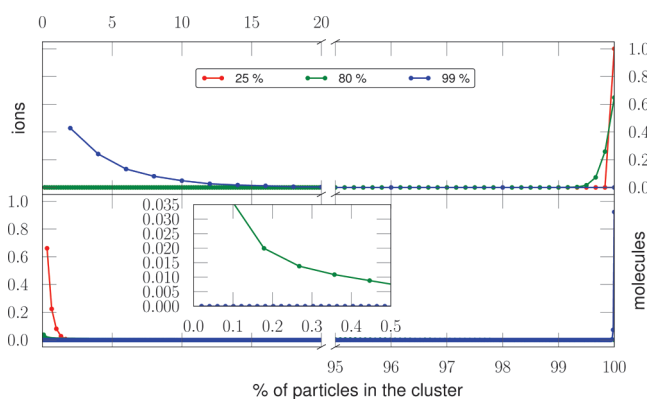


Figure 3. Probability of finding an ion (top) or a water molecule (bottom) in a cluster comprising a given percentage of the particles of that same type in the simulation box, for three different water concentrations. Solid circles mark the possible sizes: $n = 1, n = 2, \dots$, starting from the left. The inset shows the probabilities for low concentrations in greater detail.

aggregate comprising a given percentage of the particles in the simulation box, $p(\%)$, for three different water concentrations. The solid dots show the actual cluster sizes n in order $n = 1, n = 2, \dots$. The same quantities are shown for mixtures with ethanol in Figure 4; the equivalent plot for methanol is very similar and

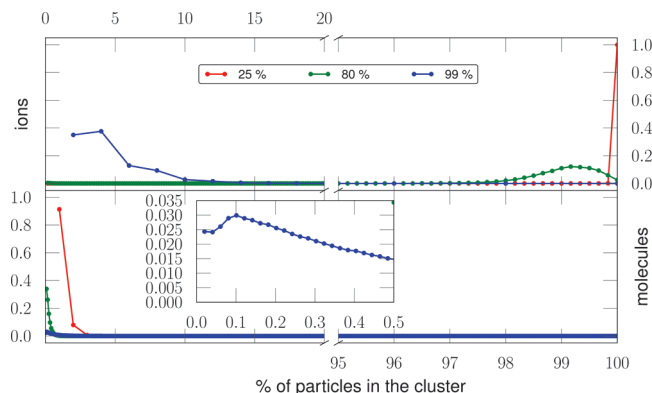


Figure 4. Probability of finding an ion (top) or an ethanol molecule (bottom) in a cluster comprising a given percentage of the particles of that same type in the simulation box, for three different ethanol concentrations. Symbols as in Figure 3. The inset shows the probabilities for low concentrations.

is thus provided as part of the Supporting Information for this paper. The broken horizontal axes in both figures serve the purposes of highlighting the lower and higher percentages and hiding the intermediate values, which were found to have negligible probability.

As Figure 3 (top) shows, the size of ionic clusters decreases when the amount of water in the mixture is increased, which is in good agreement with the results reported by Bernardes et al.²⁵ Up to a water concentration around 90%, all the ions tend to be part of the same large cluster, which can in fact be identified as a polar IL network; after this percentage the probability of finding small ionic clusters starts to increase, while at over 98% of water most of the ions are isolated within bulk water. As expected, the behavior of water molecules is exactly the opposite. As depicted in Figure 3 (top), at low water concentrations isolated water molecules or those belonging to very small clusters (no more than four or five molecules) dominate the mixture. As the amount of water increases, the probability of finding water aggregates with larger sizes starts to rise, and over a water concentration of 85% many water molecules belong to a cluster whose size is very close to the total number of water molecules in the mixture, with only a few isolated or forming small independent water clusters. The fact that most water molecules are isolated at low water concentrations is consistent with conclusions previously reported in the literature,^{21,24} and it has been attributed to the strong interaction between water molecules and anions.^{22,28} We note that there is no particular tendency to the formation of ion pairs or larger uncharged clusters in preference to single ions or charged clusters. This may be attributed to the high dielectric constant of water. Another factor behind this observation is the intermediate hydrophobicity of [BMIM]-[BF₄], since more hydrophobic ILs could be expected to prefer forming small clusters to being solvated in isolation by molecules in the mixture.

As suggested by some previous results,³⁰ the behavior of clusters in IL + alcohol mixtures is markedly different. For IL +

ethanol mixtures with 25% ethanol, Figure 4 (top) shows that the size distribution of ionic clusters shares its main features with the case of IL-water mixtures. However, as more alcohol is added (for example, at 80%), 100% of ions stops being the most frequent percentage of particles in a cluster which implies that the IL network has been broken into large ionic clusters. This intermediate regime was not observed in mixtures with water at any concentration, since in that case ions predominantly appear either isolated or forming a single IL network. It is reasonable to hypothesize that a continuous transition from a IL network to small clusters may exist, and as such there should be medium-sized clusters at some intermediate concentration, but if this is the case, the width of the transition region is too narrow for it to be detected in this kind of study. Figure 4 (top) also provides evidence of the tendency of ions to appear in pairs even at very high alkanol concentrations, such as 99% ethanol. This is reflected in the fact that the most frequent size is not $n = 1$, but $n = 2$. Histograms for the most dilute IL + methanol mixtures (included as Supporting Information) reveal that, in contrast to this, within these systems isolated ions are more likely than ionic pairs. In regard to alcohol clusters, Figure 4 (bottom) shows that, although it is true that when more alcohol is present clusters somewhat larger than a dimer become possible, an alcohol network is never formed (even in pure alcohol), in stark contrast to what happens in water. This behavior, now directly observed in the simulations, is probably at the root of the differences in equilibrium and dynamical properties of IL + water vs IL + alcohol mixtures reported in previous papers.^{30,50}

Arguably, expressing concentrations in terms of mole fractions may not be the most informative choice as regards the spatial organization of a liquid mixture. The ability of molecules to interact among themselves depends not only on their number but also on the space available to them, related, in turn, to their molar volume. This is especially important when molecules of quite different sizes are being compared, as is the case in this work. Further insight can be gained by studying aggregation as a function of the volume fraction of the molecular species, ϕ_s . By way of example, volume fraction is also considered the relevant magnitude for spatial occupation in the Flory–Huggins polymer solution theory⁵¹ and the statistical lattice theory of mixtures.⁵² Figure 5 shows the same information as Figure 2 but now presented as a function of ϕ_s . For the convenience of readers, and so as to avoid presenting equivalent revisions of other figures, a set of

equivalences between mole fractions and volume fractions are shown in Table 1. The densities used to build this table were also taken from GROMACS simulations, already proved capable of yielding reliable values of this variable.³⁰

Table 1. Volume Fraction vs Mole Fraction for the Three Molecular Species Studied

x (%)	ϕ_{water} (%)	ϕ_{methanol} (%)	ϕ_{ethanol} (%)
5	0.50	1.12	1.57
15	1.66	3.67	5.07
25	3.09	6.73	9.18
50	8.75	17.92	23.44
75	22.38	40.05	48.20
80	27.77	47.28	55.45
85	35.27	56.22	63.94
90	46.44	67.43	73.96
95	64.77	81.77	85.83
98	82.64	92.24	94.04
99	90.61	96.05	96.98

The behavior of ionic clusters is approximately universal when studied as a fraction of the volume fraction of the molecular species, due to the fact that, water molecules being smaller than alcohol molecules, $\phi_{\text{water}}(x)$ is the slowest-growing function in Table 1, which neutralizes the relatively small differences apparent in the left panels of Figure 2. On the other hand, the greater tendency of water to form clusters is even more patent in Figure 5: big clusters are clearly dominant in water from volume fractions as low as 20%, whereas for alcohols they are either totally absent (in ethanol) or present only at very high alcohol volume fractions (in methanol). Even small molecular clusters, known from our previous detailed analysis of sizes to be mainly aggregates of less than 10 molecules, appear only very gradually when alcohol is added to the mixtures, while in water they contain nearly four out of ten molecules at a volume fraction of water just over 3%.

Thus, from the analysis of cluster formation in mixtures of [BMIM][BF₄] with water, ethanol, and methanol we can conclude that when a low amount of molecular species is present in the mixture both water and alcohol molecules tend to be isolated from each other or forming clusters smaller than four or five molecules. When we add more molecular liquid to the mixture, the probability of finding larger molecular clusters increases while at the same time the probability of finding all the ions in a single large cluster forming a polar network of IL decreases, which is a sign that molecular clusters are starting to break the ionic network. Finally, at very high water concentrations water molecules tend to belong to a single large cluster whose size is approximately the same as the number of water molecules present in the mixture, showing the formation of a water network that completely breaks the ionic network, since ions tend to be isolated or forming very small clusters at this water concentration. Figure 6 illustrates this by showing the ionic clusters at a particular time step for three water concentrations. Regarding alcohols, at very high concentrations ions tend to form ion pairs in mixtures with ethanol and to be isolated if the added alkanol is methanol. This difference can be attributed to the lower dielectric constant of ethanol compared to water and methanol. Contrary to what happens in mixtures with water, very large clusters of alcohol molecules are not found at any amount of either ethanol or methanol, which suggests that alcohol molecules are

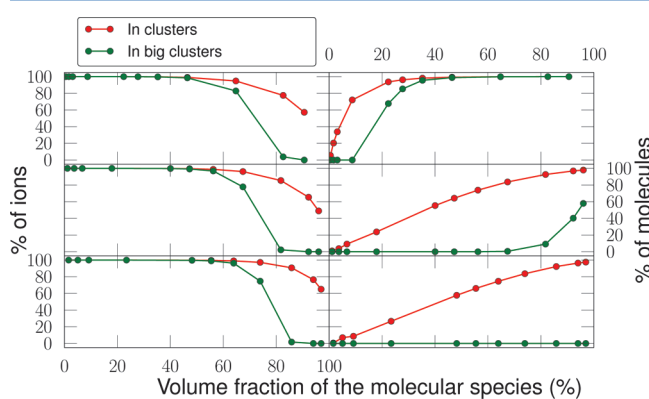


Figure 5. As Figure 2, but with the volume fraction as the independent variable. From top to bottom: water, methanol, and ethanol.

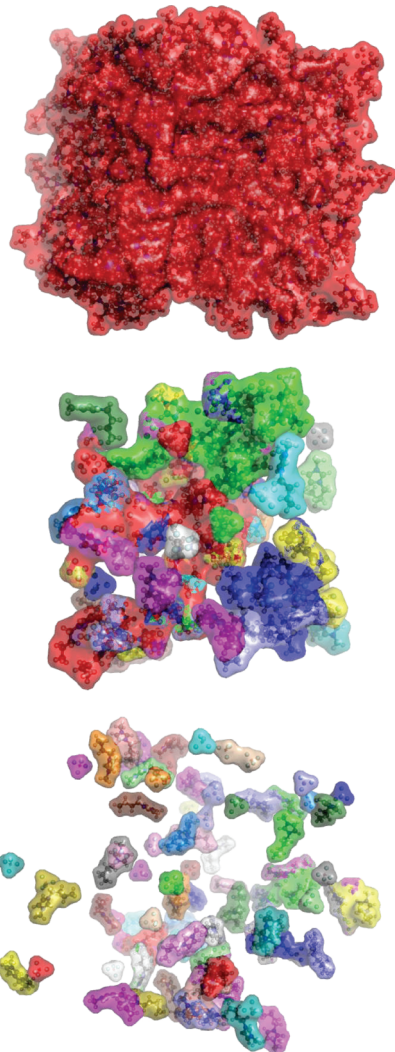


Figure 6. Ionic clusters in a $[\text{BMIM}]^+ \text{[BF}_4^-]$ + water mixture with 25% (top), 95% (center) and 99% (bottom) water. The different colors of the surfaces enclosing the clusters are intended to help differentiate them. The progressive breakdown of the ionic network can be observed.

much more homogeneously distributed in the structure of the imidazolium-based IL. This explains their reduced ability to break the IL network, reflected in the fact that an intermediate regime with large ionic clusters appears in mixtures with alcohol, but is not detected in those with water, in agreement with previously reported results.³⁰

Another way to study the structure of mixtures of $[\text{BMIM}]^+ \text{[BF}_4^-]$ with water and alcohols is the analysis of the angular distribution of molecules around the cation and the anion in the systems. To this end, we took a coordinate system centered on C2 (the carbon atom between the nitrogen atoms in the ring) for the cation or B (the central boron atom) for the anion, and computed the angle θ_1 between two vectors: the first is the position vector of the oxygen atom of the molecular species; the second goes from the oxygen atom to the middle point of the two hydrogens (in water) or to middle point between the H and C atoms bonded to the oxygen (in alcohols). This definition is shown schematically in Figure 7 for water and ethanol, the latter of which is also valid for methanol. Therefore, this second vector is parallel to the dipole moment of water, but forms an angle of 27.8° with the dipole moment of

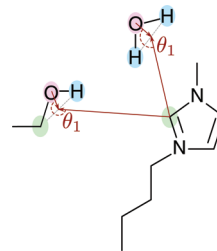


Figure 7. Graphical scheme of the definition of θ_1 for two molecules, water and ethanol, around a $[\text{BMIM}]^+$ ion. The criterion for methanol is identical to that of ethanol.

ethanol and a 47.4° angle with the dipole moment of methanol. We then proceeded to study the conditional probability density $f(\cos \theta_1 | r)$, i.e., the probability density that a molecule known to be placed at a distance r from a central ion is oriented in such a way that it yields a value of $\cos \theta_1$ in a particular interval. This density provides a detailed picture of the structure of each solvation layer of both cations and anions.

In Figures 8 and 9, we illustrate the probability density of $\cos \theta_1$ in $[\text{BMIM}]^+ \text{[BF}_4^-]$ + water mixtures for different distances and

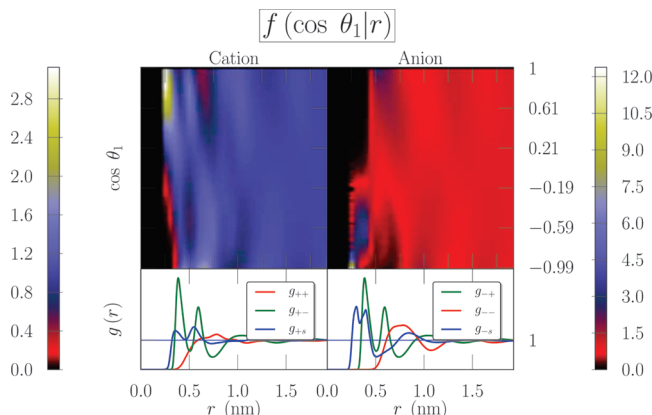


Figure 8. Conditional probability density of $\cos \theta_1$ for water molecules at different distances in mixtures of $[\text{BMIM}]^+ \text{[BF}_4^-]$ with a water concentration of 25%. Cation–cation or anion–anion (red), cation–anion (green), and ion–molecular species (blue) RDFs are also included for easy comparison.

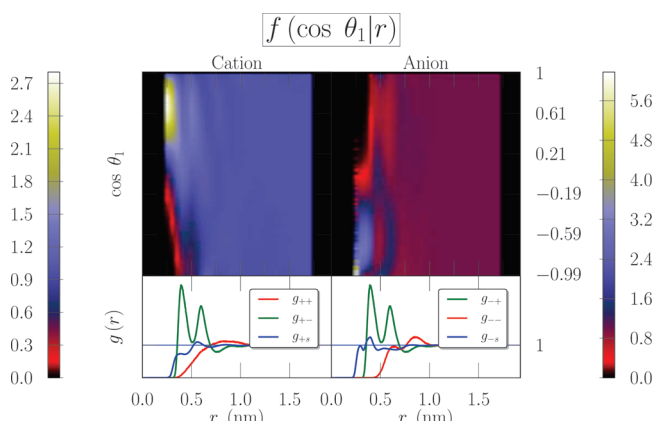


Figure 9. As in Figure 8, but for a water concentration of 95%.

two water concentrations (25% and 95%, respectively) in order to analyze the orientation of molecules around the cation (left)

and the anion (right) and its evolution with the addition of molecular liquid to the mixtures. Taking into account the definitions given above, in Figures 8 and 9 it can be seen that those water molecules placed immediately beyond the van der Waals excluded volume of the ions are closely aligned with the monopole term of the cation and anion fields, since $\cos \theta_1 = +1$ and $\cos \theta_1 = -1$, respectively. As expected from their charges, the cation prefers the region near the oxygen atom of water and far from the two hydrogen atoms, while the anion gets close to the oxygen atom approaching from between the two hydrogen atoms. Moreover, in the first solvation layer of water molecules around both the cation and the anion we observed an exclusion area, antiparallel to the field, where no water molecules can be found. In the case of the solvation of the anion, at low water concentrations there is another exclusion area around 0.5 nm in which there are no water molecules parallel to the field. However, this exclusion area disappears with the addition of water to the mixture and it can not be detected over a water concentration of 50%. This indicates that the interaction of water molecules with the anion is very strong at low water concentrations, as we reported in our previous analysis of cluster formation. Furthermore, it can be seen that as we add water to the mixture the former is less oriented around the ions (the maximum of the probability density is more diffuse and not so clearly placed at $\cos \theta_1 = \pm 1$) since water molecules tend to interact more strongly with each other than with the charged ions. This is a sign of the formation of water clusters in mixtures of $[\text{BMIM}]^+[\text{BF}_4]^-$ and water.

In Figures 10 and 11, it can be seen that the behavior of ethanol molecules is completely different from that of water.

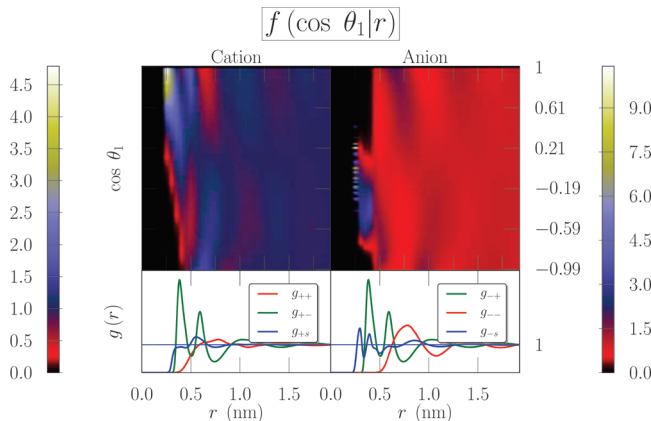


Figure 10. As in Figure 8, but for ethanol molecules in a $[\text{BMIM}]^+[\text{BF}_4]^-$ + ethanol mixture with 25% ethanol.

First, while in the solvation layer of the cation there is also an area without alcohol molecules parallel to the field, the orientation of alcohol molecules around the anion shows two exclusion zones, in one of them the alcohol molecules being parallel to the field and in the other antiparallel. Additionally, looking at the orientation of alcohol molecules around the anion, it can be seen that in the first solvation shell (presumably with the anion near the oxygen atom) several discrete orientations are possible, probably due to the presence of cations in the neighborhood, whose chains interact with the alcohol molecules, favoring only a certain number of angles. Moreover, the second layer seems to be more oriented than the first one. Finally, the orientation of alcohol molecules around both ions experiences almost no changes with the addition of

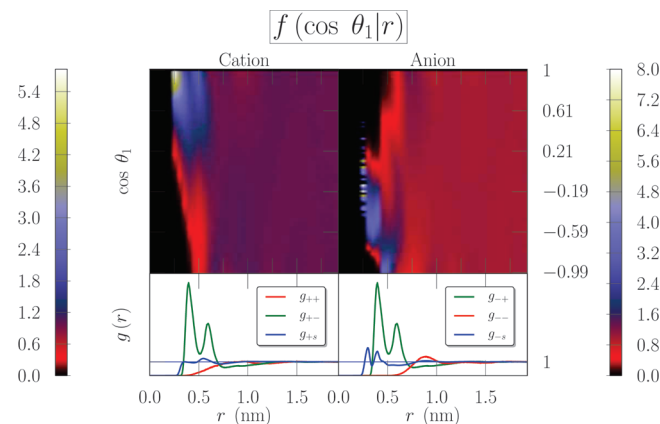


Figure 11. As in Figure 8, but for ethanol molecules in a $[\text{BMIM}]^+[\text{BF}_4]^-$ + ethanol mixture with 95% ethanol.

alcohol to the mixture, which shows that alcohol distribution in bulk mixtures depends only slightly on the concentration, in agreement with our previous statement that alcohol molecules do not form large aggregates in the mixture. The results for methanol are similar, albeit with a narrower distribution of orientations around the anion. The corresponding figures are provided as Supporting Information.

Since the limited ability of ethanol and methanol to form hydrogen bonds impedes cluster formation, we looked for subtler clues about the structure of these alcohols in mixtures with ILs. One such clue is provided by the atomistic RDFs shown in Figure 12, where the first group considered comprises

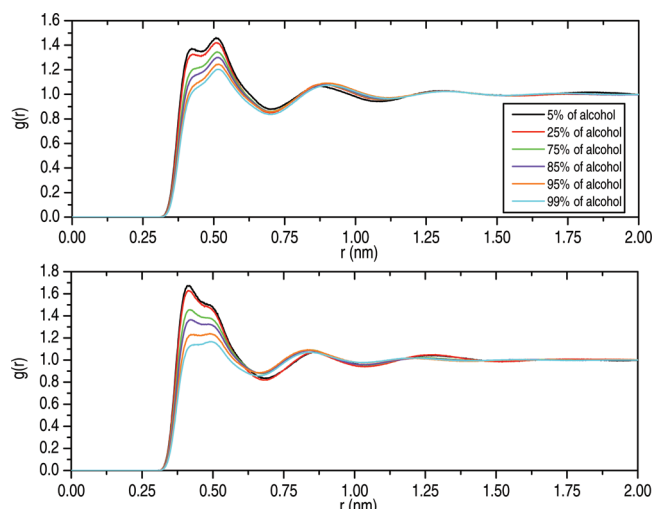


Figure 12. Atomistic RDF of the carbons in the alcohol with respect to those in the alkyl side chain of $[\text{BMIM}]^+$, for six different mole fractions of ethanol (top) and methanol (bottom).

the carbon atoms in the alkyl side chain of $[\text{BMIM}]^+$ and the second group is formed by the carbon atom (both carbon atoms) of methanol (ethanol). Therefore, Figure 12 contains information about the distribution of distances between the apolar parts of both the IL and the alkanol in $[\text{BMIM}]^+[\text{BF}_4]^-$ + alcohol mixtures. Not unexpectedly, there is a tendency for apolar chains to stick together, manifested in the sheer rise of these RDFs right after the excluded region. The broad width of the peaks in Figure 12 is explained by the fact that carbons in the alcohol can be close to any of the four carbons in the alkyl

chain of the IL, the most extreme of which are separated by 0.38 nm. This small degree of structure is gradually lost as more alcohol is added and alcohol–alcohol interactions become more relevant in detriment of alcohol-IL interactions.

Finally, some order could be expected to exist in alcohols due to dipole interactions, which should result in the formation of structures consisting of predominantly parallel alcohol molecules, rather than clusters. In a mixture with N_a molecules of alcohol, each with a dipole moment μ , a standard variable used to study the degree to which a random molecular dipole μ_j inside a sphere of radius r with its center on another random dipole μ_i is (on average) oriented at random or aligned parallel to μ_i is the Kirkwood G factor,⁵³

$$G_K(r) = \frac{1}{N_a \mu^2} \sum_{i,j} \mu_i \cdot \mu_j \left| r_{ij} < r \right| \quad (2)$$

G_K can also be calculated as an integral⁵³

$$G_K(r) = 1 + \frac{4\pi}{3V} N_a \int_0^r h_\Delta(R) R^2 dR \quad (3a)$$

with

$$h_\Delta(r) = 3g_{OO}(r) \langle \cos \theta \rangle \quad (3b)$$

Here, $g_{OO}(r)$ is the RDF for alcohol oxygen atoms and $\langle \cos \theta \rangle$ the average cosine of the angle between two dipoles at distance r . Thus, $h_\Delta(r)$ is an indicator of the tendency to parallelism of alcohol molecules at a particular distance. Figure 13 shows both

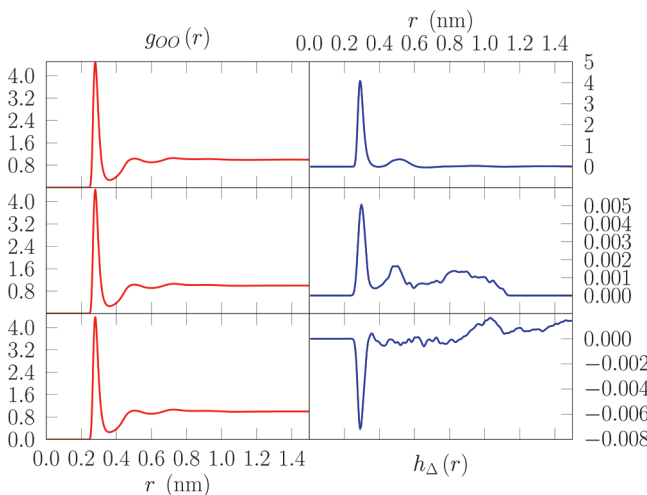


Figure 13. Oxygen–oxygen RDF and h_Δ (see definition in the text) for ethanol molecules in pure ethanol (top) and in mixtures with $[BMIM][BF_4]$ at two different mole fractions of ethanol: 99% (center) and 98% (bottom).

$g_{OO}(r)$ and $h_\Delta(r)$ for pure ethanol (top) and for its mixtures with $[BMIM][BF_4]$ at two different mole fractions of ethanol: 99% (center) and 98% (bottom). The contrast between the behavior of both variables is noteworthy, since while the oxygen–oxygen RDF is essentially identical for any of the three concentrations, h_Δ falls by 3 orders of magnitude even when just a tiny amount of IL is added to pure ethanol. In physical term, this means that the angular correlation that is detected in pure ethanol, induced by dipole interactions, is almost completely destroyed by the monopole field of ions. Furthermore, at 98% ethanol it can be seen that $g_{OO}(r)$ and

h_Δ have opposite signs around the first peak of the former, a sign that even neighboring ethanol molecules are more influenced by whatever ion they are solvating than by each other. This trend continues at lower concentrations not shown in Figure 13. Equivalent conclusions can be drawn from the corresponding figure for methanol, which is provided as Supporting Information, except that h_Δ does not change sign even at lower alcohol concentrations. This is probably due to the greater relative importance of the polar part in methanol with respect to ethanol.

It must be noted that, even for ethanol, in those mixtures with a high concentration of the molecular species, and particularly in the pure molecular liquid, it is possible to trace a straight path from one molecule to the nearest neighbor of its kind with a low probability of intersection an ion. In other words, the existence of connected regions rich in the molecular species is ineluctable, due to the sheer difference in numbers of molecules vs ions. Nevertheless, these regions are not clusters in the sense that this work concerns itself with—those formed by molecules or ions interacting through particular kinds of physical forces. Beyond the 0.35 nm cutoff distance used in this paper, the neighborhood relations in pure ethanol and methanol have been studied in great detail in a separate work³⁰ though the use of partial RDFs; judging by the fact that g_{OO} is not appreciably changed by the addition of a few ions, the results in Figure 10 of ref 30 can be expected to also provide an accurate description of alcohol-rich mixtures. Those partial RDFs also reflect a much more disorganized environment around ethanol molecules than in the case of methanol, due to the greater competence between polar and hydrophobic interactions.

CONCLUSIONS

We performed MD simulations for mixtures of an imidazolium-based IL, $[BMIM][BF_4]$, with three different molecular species, water and two alcohols of different chain lengths (methanol and ethanol), and we investigated the formation of clusters of ions or molecules within these systems, as well as the orientation of molecules around the cation and the anion of the IL.

The criterion to decide if two molecules or a cation and an anion were bonded and belonged to the same cluster was based on the study of the RDFs. In the case of the molecular species, we took as the clustering cutoff the distance at which the first minimum of the RDF oxygen–oxygen for the pure molecular liquid was located. For ionic clusters, to take heterocoordination into account we chose to consider that a cation and an anion formed part of the same aggregate if the distance between them was shorter than the distance at which the cation–anion ($C_2–B$) and cation–cation ($C_2–C_2$) radial distribution functions intersect. The results of these calculations show that the polar network of IL is gradually broken with the addition of any of the three molecular species, resulting in most of ions becoming isolated (in water or methanol) or forming ionic pairs (in the case of ethanol) at very high concentrations of the molecular liquids. However, there are important differences in behavior between water and alcohols: in mixtures with water we found that at low water concentrations water molecules tend to be isolated or form part of small clusters (with no more than four or five molecules) due to their strong interaction with the anion, while at high water concentrations water molecules form very large aggregates that give rise to a water network; in contrast, in mixtures with either methanol or

ethanol there is no evidence of the formation of large alcohol clusters even when very high amounts of alcohol are added to the mixture; instead, alcohol molecules are much more homogeneously placed in the structure of the imidazolium-based IL. These results are in good agreement with those reported in our previous work.³⁰

We also looked for subtler signs of ordering in mixtures of [BMIM][BF₄] with alcohols. Our analysis of the RDFs of the apolar part of the alcohols with respect to the apolar part [BMIM] shows some signs of structure due to hydrophobic interactions. On the other hand, any angular correlation between alcohol molecules, which is clearly present in pure alcohols due to dipole interactions, is destroyed by the introduction in the system of even a few ions. As a consequence, very little medium- or long-range order persists in such mixtures.

Furthermore, in our analysis of the orientation of molecules around the cation and the anion, we found that the angular distribution of water molecules around the ions changes with the addition of water, with water molecules becoming less oriented along the field lines of the ions as we add water to the mixture. This shows that at high water concentrations water molecules tend to form large clusters inside which they interact with each other in a bulk-like fashion in preference to interacting with the ions, which is the behavior at low water concentrations. In contrast, in mixtures with both alcohols the orientation of alcohol molecules around the ions does not change in a significant way with the addition of alcohol, which is a sign that the structure of alcohol in these systems does not depend substantially on the amount of alcohol present, as alcohols do not form large clusters at any concentration.

A similar study of the aggregation process and the angular orientation in mixtures of imidazolium-based ILs with lithium and sodium salts is now in progress. Another line of work we are pursuing is the study of the influence of the hydrophobicity of the ionic liquid on cluster formation, especially as regards the relative abundance of isolated ions vs ionic pairs or other small clusters.

■ ASSOCIATED CONTENT

Supporting Information

Figures equivalent to Figures 3, 8, 9, and 13, for [BMIM][BF₄] + methanol mixtures. This material is available free of charge via the Internet at <http://pubs.acs.org/>.

■ AUTHOR INFORMATION

Corresponding Author

*E-mail: luismiguel.varela@usc.es.

Notes

The authors declare no competing financial interest.

■ ACKNOWLEDGMENTS

The authors express thanks for the financial support of Xunta de Galicia through the research projects of references 10-PXI-103-294 PR, 10-PXIB-206-294 PR, and INCITE10PXIB206294 PR. Moreover, this work was funded by the Spanish Ministry of Science and Innovation (Grant No. FIS2008-04894/FIS). All these research projects are partially supported by FEDER. T.M.-M. and J.C. thank the Spanish Ministry of Education for their FPU grants. Facilities provided by the Galician Supercomputing Centre (CESGA) are also acknowledged.

■ REFERENCES

- (1) Rogers, R. D.; Seddon, K. R. *Science* **2003**, *302*, 792–793.
- (2) Wilkes, J. S. *Green Chem.* **2002**, *4*, 73–80.
- (3) Huddleston, J. G.; Visser, A. E.; Reichert, W. M.; Willauer, H. D.; Broker, G. A.; Rogers, R. D. *Green Chem.* **2001**, *3*, 156–164.
- (4) Earle, M. J.; Seddon, K. R. *Pure Appl. Chem.* **2000**, *72*, 1391–1398.
- (5) Holbrey, J. D.; Seddon, K. R. *Clean Prod. Proc.* **1999**, *1*, 223–236.
- (6) Welton, T. *Chem. Rev.* **1999**, *99*, 2071–2084.
- (7) Wasserscheid, P.; Keim, M. *Angew. Chem., Int. Ed. Engl.* **2000**, *39*, 3772–3789.
- (8) Rogers, R. D.; Seddon, K. R. *Ionic liquids as green solvents: progress and prospects*; American Chemical Society: Washington, DC, 2003.
- (9) Hagiwara, R.; Ito, Y. *J. Fluorine Chem.* **2000**, *105*, 221–227.
- (10) Wasserscheid, P.; Welton, T. *Ionic liquids in synthesis*; Wiley Online Library: 2003.
- (11) Rogers, R. D.; Seddon, K. R. *Ionic liquids: industrial applications for green chemistry*; American Chemical Society: 2002.
- (12) Zhao, Y.; Chen, Z.; Wang, J.; Zhuo, K. *Z. Phys. Chem.* **2009**, *223*, 857–868.
- (13) Pereiro, A. B.; Rodriguez, A. *J. Chem. Thermodyn.* **2007**, *39*, 978–989.
- (14) Seddon, K. R.; Stark, A.; Torres, M. J. *Pure Appl. Chem.* **2000**, *72*, 2275–2287.
- (15) Rebelo, L. P. N.; Najdanovic-Visak, V.; Visak, Z. P.; da Ponte, M. N.; Szydlowska, J.; Cerdeirinha, C. A.; Troncoso, J.; Roman, L.; Esperanca, J. M. S. S.; Guedes, H. J. R.; de Sousa, H. C. *Green Chem.* **2004**, *6*, 369–381.
- (16) Najdanovic-Visak, V.; Esperanca, J. M. S. S.; Rebelo, L. P. N.; da Ponte, M. N.; Guedes, H. J. R.; Seddon, K. R.; de Sousa, H. C.; Szydlowski, J. *J. Phys. Chem. B* **2003**, *107*, 12797–12807.
- (17) Kelkar, M. S.; Maginn, E. J. *J. Phys. Chem. B* **2007**, *111*, 4867–4876.
- (18) Carrete, J.; Garca, M.; Rodriguez, J.; Cabeza, O.; Varela, L. *Fluid Phase Equilib.* **2011**, *301*, 118–122.
- (19) Cuadrado-Prado, S.; Domnguez-Pérez, M.; Rilo, E.; Garca-Garabal, S.; Segade, L.; C. Franjo, O. C. *Fluid Phase Equilib.* **2009**, *278*, 36–40.
- (20) Cammarata, L.; Kazarian, S. G.; Salter, P. A.; Welton, T. *Phys. Chem. Chem. Phys.* **2001**, *3*, 5192–5200.
- (21) Fazio, B.; Triolo, A.; Marco, G. D. *J. Raman Spectrosc.* **2008**, *39*, 233–237.
- (22) Takamuku, T.; Kyoshin, Y.; Shimomura, T.; Kittaka, S.; Yamaguchi, T. *J. Phys. Chem. B* **2009**, *113*, 10817–10824.
- (23) Zhang, L.; Xu, Z.; Wang, Y.; Li, H. *J. Phys. Chem. B* **2008**, *112*, 6411–6419.
- (24) Hanke, C. G.; Lynden-Bell, R. M. *J. Phys. Chem. B* **2003**, *107*, 10873–10878.
- (25) Bernardes, C. E. S.; da Piedade, M. E. M.; Canongia-Lopes, J. N. *J. Phys. Chem. B* **2011**, *115*, 2067–2074.
- (26) Feng, S.; Voth, G. A. *Fluid Phase Equilib.* **2010**, *294*, 148–156.
- (27) Jiang, W.; Wang, Y.; Voth, G. A. *J. Phys. Chem. B* **2007**, *111*, 4812–4818.
- (28) Moreno, M.; Castiglione, F.; Mele, A.; Pasqui, C.; Raos, G. *J. Phys. Chem. B* **2008**, *112*, 7826–7836.
- (29) Spickermann, C.; Thar, J.; Lehmann, S. B. C.; Zahn, S.; Hunger, J.; Buchner, R.; Hunt, P. A.; Welton, T.; Kirchner, B. *J. Chem. Phys.* **2008**, *129*, 104505(1)–104505(13).
- (30) Méndez-Morales, T.; Carrete, J.; Cabeza, O.; Gallego, L. J.; Varela, L. M. *J. Phys. Chem. B* **2011**, *115*, 11170–11182.
- (31) Canongia-Lopes, J. N.; Costa-Gomes, M. F.; Padúa, A. A. H. *J. Phys. Chem. B* **2006**, *110*, 16816–16818.
- (32) Spoel, D. V. D.; Lindahl, E.; Hess, B.; Buuren, A. R. V.; Apol, E.; Meulenhoff, P. J.; Tielemans, D. P.; Sijbers, A. L. T. M.; Feenstra, K. A.; Drunen, R. V.; Berendsen, H. J. C. *Gromacs User Manual version 4.0*; <http://www.Gromacs.org>, 2005
- (33) Anthony, J. L.; Maginn, E. J.; Brennecke, J. F. *J. Phys. Chem. B* **2001**, *105*, 10942–10949.

- (34) Domańska, U.; Marciniak, A. *J. Phys. Chem. B* **2004**, *108*, 2376–2382.
- (35) Crosthwaite, J. M.; Aki, S. N. V. K.; Maginn, E. J.; Brennecke, J. F. *J. Phys. Chem. B* **2004**, *108*, 5113–5119.
- (36) Rilo, E.; Pico, J.; Garca-Garabal, S.; Varela, L. M.; Cabeza, O. *Fluid Phase Equilib.* **2009**, *285*, 83–89.
- (37) Jorgensen, W. L. *J. Phys. Chem.* **1986**, *90*, 1276–1284.
- (38) Prado, C. E. R.; Freitas, L. C. G. *J. Mol. Struct. (THEOCHEM)* **2007**, *847*, 93–100.
- (39) Brenneman, C. M.; Wiberg, K. B. *J. Comput. Chem.* **1990**, *11*, 361–373.
- (40) Frisch, M. J. et al. *Gaussian 94, Revision A.1*; Gaussian, Inc.: Pittsburgh, PA, 1995.
- (41) Mahoney, M. W.; Jorgensen, W. L. *J. Chem. Phys.* **2000**, *112*, 8910–8922.
- (42) Jorgensen, W. L.; Maxwell, D. S.; Tirado-Rives, J. *J. Am. Chem. Soc.* **1996**, *118*, 11225–11236.
- (43) Darden, T.; York, D.; Pedersen, L. *J. Chem. Phys.* **1993**, *98*, 10089–10094.
- (44) Hess, B.; Bekker, H.; Berendsen, H. J. C.; Fraaije, J. G. E. M. *J. Comput. Chem.* **1997**, *18*, 1463–1472.
- (45) Hess, B. *J. Chem. Theory Comp.* **2007**, *4*, 116–122.
- (46) Micalo, N. M.; Baptista, A. M.; Soares, C. M. *J. Phys. Chem. B* **2006**, *110*, 14444–14451.
- (47) Bussi, G.; Donadio, D.; Parrinello, M. *J. Chem. Phys.* **2007**, *126*, 014101(1)–014101(7).
- (48) Parrinello, M.; Rahman, A. *J. Appl. Phys.* **1981**, *52*, 7182–7190.
- (49) Haughney, M.; Ferrario, M.; McDonald, I. R. *J. Phys. Chem.* **1987**, *91*, 4934–4940.
- (50) Méndez-Morales, T.; Carrete, J.; García, M.; Cabeza, O.; Gallego, L. J.; Varela, L. M. *J. Phys. Chem. B* **2011**, *115*, 15322–15322.
- (51) Flory, P. J. *Principles of Polymer Chemistry*; Cornell University Press: Ithaca, NY, 1953.
- (52) Lacombe, R. H.; Sanchez, I. *J. Phys. Chem.* **1976**, *80*, 2568–2580.
- (53) Nymand, T. M.; Linse, P. *J. Chem. Phys.* **2000**, *112*, 6386–6395.